Table 1 Target pathogens and specific primers

Well	Pathogen	Target gene	Forward primer	Reverse primer	Amplicon (bp)
1A	*Neisseria gonorrhoeae*	16S rDNA	5′-GCATACGTCTTGAGAGRGAA-3′	5′-ACACTCGAGTCACCCAGTTC-3′	482
1B	*Chlamydia trachomatis*	16S rDNA	5′-TGGCGGCGTGGATGAGGCAT-3′	5′-CTCAGTCCCAGTGTTGGCGG-3′	300
1C	*Mycoplasma genitalium*	16S rRNA	5′-GCACCTGCAAGGGTTCGTTA-3′	5′-ACAACTGTTAAGCAGCTGCC-3′	420
1D	*Mycoplasma hominis*	16S rDNA	5′-AGGTTAGCAATAACCTAGCG-3′	5′-GTACCGTCAGTCTGCAATC-3′	417
1E	*Mycoplasma fermentans*	IS-like element	5′-GGACTATTGTCTAAACAATTTCCC-3′	5′-GGTTATTCGATTTCTAAATCGCCT-3′	206
1F	*Treponema pallidum*	16S rDNA	5′-GTAATCTGCCTTTGAGATGG-3′	5′-CCAGTGTGTCCGGTCACCCT-3′	203
1G	*Tricomonas vaginalis*	18S rDNA	5′-TAATGGCAGAATCTTTGGAG-3′	5′-GAACTTTAACCGAAGGACTTC-3′	312
1H	*Ureaplasma urealyticum*	16S rDNA	5′-CAAATCGAACGAAGCCTTT-3′	5′-TTTTGATACAGCTAGACGTTA-3′	593
2A	*Haemophilus ducreyi*	16S rRNA	5′-CGGTAGCACGAAGGGGTTGC-3′	5′-GCTATTAACAAAACTGCCTT-3′	390
2B	*Haemophilus influenzae*	16S rDNA	5′-AGCAGGAGRAAGCTTGCTTTC-3′	5′-CCTTCCTCAATACCGAAAGA-3′	397
2C	*Haemophilus parainfluenzae*	16S rDNA	5′-AGTAATGCTTGGGAATCT-3′	5′-TGGGCCGTGTCTCAGTCC-3′	222
2D	*Bacteroides ureolyticus*	16S rDNA	5′-GTAAGGTAATGGCTTACCAAG-3′	5′-TCATTATTCTTTCCTGATAA-3′	210
2E	*Streptococcus agalactiae*	16S rDNA	5′-GCGAAAGCGGCTCTCTGGTC-3′	5′-GCTTTCTCTTCGGAGCAGAA-3′	316
2F	*Klebsiella pneumoniae*	16S rDNA	5′-GGTTGTGCCCTTGAGGCGT-3′	5′-CCATGCA(T/G)CACCTGTCTCAC-3′	227
2G	Herpes simplex virus I/II (HSV)	Glycoprotein B	5′-CTGGTCAGCTTTCGGTACGA-3′	5′-AGGTCGATGAAGGTGCTGACGGTGGTGA-3′	218
2H	Human papilloma virus (HPV)	Capsid protein	5′-TGTCAAAAGCCACTGTGTCC-3′	5′-GAGCTGTCACTTAATTGCTC-3′	250

bp, base pair; rDNA, ribosomal DNA.

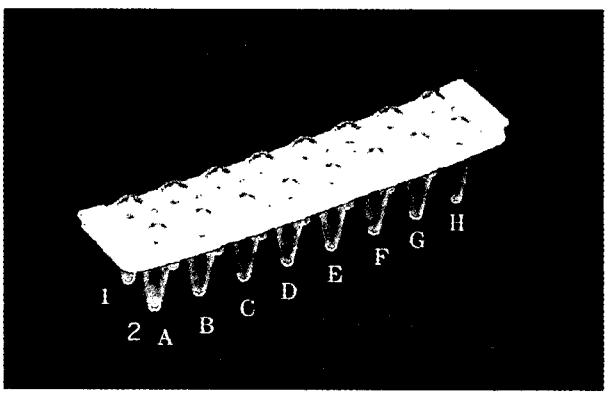

Fig. 1 Image of the covered 16-well microplate used in the present study.

patients provided informed consent for their participation. All patients had symptoms and signs consistent with acute urethritis. A diagnosis of urethritis was based on the observation of five or more polymorphonuclear leukocytes per oil-immersion field (×1000) in a Gram-stained endourethral swab specimen. Clinical samples were collected as follows: urethral exudates or endourethral samples were taken with a cotton swab (Becton Dickinson, Franklin Lake, NJ, USA) inserted 3–4 cm into the urethra. These samples were dipped into a 1.5-mL microcentrifuge tube containing 500 μL TE buffer and stored at −80°C immediately. Thawed samples were boiled at 100°C for 10 min, cooled on ice for 5 min and centrifuged at 15 000 *g* for 5 min. In the last step, the top clear layer, which contained DNA, was collected. We used these DNA as templates. We confirmed that our primers did not react some specimens from non-urethritis patients as negative controls.

Sensitivity and specificity of this system for clinical samples

We compared the sensitivities and specificities of our primers for *Neisseria gonorrhoeae* and *C. trachomatis* with Amplicor STD-1[10,11] (Roche Diagnostics Systems, Indianapolis, IN, USA) and for *M. genitalium*, *M. hominis* and *U. urealyticum* with a PCR-Microtiter Plate Hybridization Assay (Mitsubishi Kagaku Bio-Clinical Laboratories, Tokyo, Japan).[5]

Results

To improve detection and identification of pathogens associated with urethritis, we developed an RT–PCR assay that allows simultaneous detection of 16 known urethritis pathogens.

The detection limits of the individual PCR were determined by serial dilutions of plasmids containing pathogen DNA. Tm, slope and intercept of the standard curve and correlation coefficient of the 16 specific primers for quantification are shown in Table 2. Representative data from *N. gonorrhoeae* (16S) are shown in Figure 2. To confirm the result of the RT–PCR assay, the PCR products were analyzed by gel electrophoresis, and the sizes of the products were compared to those of the predicted amplicons.

We did not observe any cross-reaction of any primer with DNA other than its target.

Distribution of the urethritis pathogens detected in 163 clinical samples is shown in Table 3. Ninety-two samples contained *N. gonorrhoeae*, *C. trachomatis*, *M. genitalium*, *M. hominis* or *U. urealyticum* or a mixture of these pathogens. The percentages of GU and NGU were 32.5% (53/163) and 23.9% (39/163), respectively. The mixed infection rate was 6.7% (11/163). These five pathogens were not detected in 71 cases, although urethritis was diagnosed clinically in all cases.

Table 2 Melting temperatures and standard curves for urethritis pathogen

Pathogen	Detection limit (copy number/reaction)	Melting temperature (Tm)	Slope (a) and intercept (b) Y = aX + b	Correlation coefficient	GGS number
N. gonorrhoeae (16S)	5.20×10^{-1}	92.5 ± 0.5	Y = −3.72 X + 37.26	1	1938
C. trachomatis	1.75×10^{0}	88.5 ± 0.5	Y = −3.10 X + 28.93	0.98	1931
M. genitalium (16S)	3.20×10^{-1}	89.0 ± 0.5	Y = −3.72 X + 38.23	1	1937
M. hominis	2.00×10^{0}	90.0 ± 0.5	Y = −3.36 X + 39.27	0.94	1936
M. fermentans	4.00×10^{-1}	82.0 ± 0.5	Y = −3.23 X + 38.81	0.98	1934
T. pallidum	5.56×10^{4}	91.0 ± 0.5	Y = −3.72 X + 33.88	0.99	1940
T. vaginalis	4.00×10^{-1}	89.5 ± 0.5	Y = −4.52 X + 38.62	0.99	1941
U. urealyticum	3.03×10^{-1}	90.0 ± 0.5	Y = −3.31 X + 29.49	0.98	1942
H. ducreyi	1.00×10^{0}	91.0 ± 0.5	Y = −3.12 X + 28.32	0.98	1932
H. influenzae	0.99×10^{-1}	91.5 ± 0.5	Y = −2.75 X + 36.58	0.95	1933
H. parainfluenzae	4.00×10^{-1}	89.0 ± 0.5	Y = −2.66 X + 49.12	0.95	1939
B. ureolyticus	5.64×10^{-1}	90.0 ± 0.5	Y = −2.79 X + 35.61	0.86	1929
S. agalactiae	8.40×10^{-1}	91.0 ± 0.5	Y = −3.66 X + 32.52	1	677
K. pneumoniae	4.00×10^{-1}	91.0 ± 0.5	Y = −2.88 X + 34.08	0.98	1412
HSV	1.19×10	94.0 ± 0.5	Y = −3.36 X + 32.16	0.99	1943
HPV	2.30×10^{2}	88.0 ± 0.5	Y = −3.47 X + 34.15	0.98	1940

16S, 16S ribosomal DNA; GGS, Gifu Genetic Strain.

Table 3 Distribution of urethritis pathogens in clinical samples

	Pathogens	No. (%)
GU	*N. gonorrhoeae*	44 (27.0)
	N. gonorrhoeae + *C. trachomatis*	5 (3.1)
	N. gonorrhoeae + *C. trachomatis* + *U. urealyticum*	1 (0.6)
	N. gonorrhoeae + *U. urealyticum*	3 (1.8)
NGU	*C. trachomatis*	29 (17.8)
	M. genitalium	3 (1.8)
	M. hominis	1 (0.6)
	U. urealyticum	4 (2.5)
	C. trachomatis + *U. urealyticum*	1 (0.6)
	M. hominis + *U. urealyticum*	1 (0.6)
	Negative	71 (43.6)
	Total	163

GU, gonococcal urethritis; NGU, non-gonococcal urethritis.

The sensitivity and specificity of each primer for *N. gonorrhoeae*, *C. trachomatis*, *M. genitalium* and *U. urealyticum* was more than 90% (Table 4).

Discussion

In the present study described herein, the causative pathogen in 43.6% of urethritis cases remained unknown because established pathogens were not isolated. It was recently reported that the frequency of NGU has increased, whereas the frequency of GU has decreased.[2,3] We believe that it is important to clarify the causative pathogens of NGU.

Polymerase chain reaction-based methods are often used for identification of urethritis pathogens. RT–PCR assays for *N. gonorrhoeae*, *M. genitalium*, *M. hominis*, HSV and *T. vaginalis* have been reported.[12–17] However, a system for simultaneous detection of several urethritis pathogens has not been described. The greatest advantage of RT–PCR is the speed with which one can obtain results. The iCycler iQ (Bio-Rad) can hold 96 PCR tubes or six 16-well microplates.

The limits of detection of our assay for specific pathogens except *T. pallidum* were satisfactory. A more sensitive primer for this pathogen

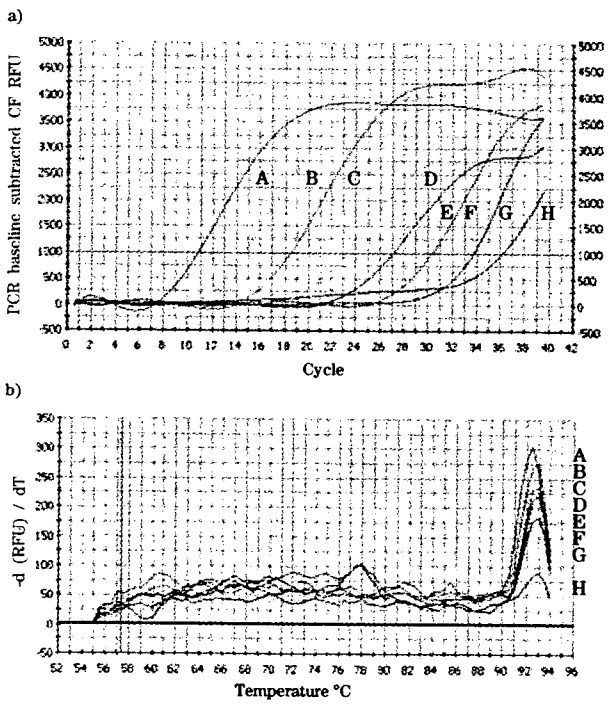

Fig. 2 Amplification curve and melting curve of *Neisseria gonorrhoeae*. We made a 10-fold dilution series of template DNA (1×10^{0} to 1×10^{-7} ng/μL, A to G, respectively, in Fig. 1). Melting temperature (Tm) was 92.5–93°C.

Table 4 Primer sensitivity and specificity for 163 clinical samples

Primer	Sensitivity (%)	Specificity (%)
N. gonorrhoeae (16S)	52/53 (98.1)	109/110 (99.1)
C. trachomatis	30/30 (100.0)	132/132 (100)
M. genitalium (16S)	3/3 (100.0)	158/160 (98.8)
M. hominis	1/2 (50.0)	161/161 (100)
U. urealyticum	9/10 (90.0)	152/153 (100)

16S, 16S ribosomal DNA.

should be designed. Multiplex RT–PCR with these specific primers did not yield satisfactory results (data not shown). If the Tm for each amplicon is too close to that of other amplicons, we cannot identify the pathogen on the basis of the Tm and, therefore, the identity of the pathogen needs to be confirmed by analysis of the PCR products by electrophoresis or another method. Furthermore, when several primers were mixed for multiplex PCR, the detection limits were not as low as those for individual primers.

According to one report, screening of 2101 urethritis patients detected *N. gonorrhoeae* in 4.6%, Chlamydia species in 14.6%, *U. urealyticum* in 25.0%, Candida species in 8.8%, *Streptococcus agalactiae* in 7.85%, *M. hominis* in 4.2%, Haemophilus species in 3.19%, *T. vaginalis* in 1.1%, HSV in 0.1% and mixed infection in 3.9%.[18] However, no causative pathogen could be identified for 35.0% of the urethritis patients with no microorganism identified.[18] In our clinical specimens, the mixed infection rate was 6.7% (11/163), and the unidentified microorganism rate was 43.6% (71/163). Our mixed infection rate was higher than that of the previous report; however, the unidentified rate was similar. There are reports that *T. vaginalis* is associated with NGU in men.[15,19] HPV is recognized as a pathogen that causes condyloma acuminatum, penile cancer and cervical cancer. The reported rate of HPV detection in urethritis patients is high,[20] suggesting that HPV may be associated with urethritis. *Mycoplasma fermentans* is also often found in the genital tract.[9]

We developed a system for simultaneous detection of 16 pathogens related to urethritis by RT–PCR. Using this system, we were able to determine the frequency of five urethritis-associated pathogens in clinical specimens. These sensitivities and specificities of our primers were satisfactory in comparison with those of reported primers.

Acknowledgments

We thank Shin-ichi Maeda, MD, PhD (Department of Urology, Toyota Memorial Hospital) for collecting clinical specimens, Kawamura Yoshiaki, PhD (Departments of Microbiology, Gifu University Graduate School of Medicine) for helpful discussion and comment and Mika Hayashi (Department of Urology, Gifu University Graduate School of Medicine) for technical assistance.

References

1 Martin DH, Bowie WR. Urethritis in males. In: Holmes KK, Mardh PA, Sparling PF *et al.* (eds). *Sexually Transmitted Diseases*, 3rd edn. McGraw-Hill, New York, 1999; 833–44.

2 Hughes G, Fenton KA. Recent trends in gonorrhoea: an emerging public health issue? *Euro. Surveill.* 2002; **5**: 1–2.

3 Goulet V, Sadnaoui P, Laporte A, Billy C, Desenclos JC. The number of gonococcal infections identified by the RENAGO network is increasing. *Euro. Surveill.* 2000; **5**: 2–5.

4 Deguchi T, Maeda S. *Mycoplasma genitalium*: another important pathogen of nongonococcal urethritis. *J. Urol.* 2002; **167**: 1210–17.

5 Yoshida T, Maeda S, Deguchi T, Miyazawa T, Ishiko H. Rapid detection of *Mycoplasma genitalium*, *Mycoplasma hominis*, *Ureaplasma parvum*, and *Ureaplasma urealyticum* organisms in genitourinary samples by PCR-microtiter plate hybridization assay. *J. Clin. Microbiol.* 2003; **41**: 1850–5.

6 Taylor-Robinson D, Furr PM. Update on sexually transmitted mycoplasmas. *Lancet* 1998; **351**: 12–15.

7 Sriprakash KS, Macavoy ES. Characterization and sequence of plasmid from the trachoma biovar of *Chlamydia trachomatis*. *Plasmid* 1987; **18**: 205–14.

8 Ho BS, Feng WG, Wong BK, Egglestone SI. Polymerase chain reaction for the detection of *N. gonorrhoeae* in clinical samples. *J. Clin. Pathol.* 1992; **45**: 439–42.

9 Crotchfelt KA, Welsh LE, DeBonville D, Rosenstraus M, Quinn TC. Detection of *N. gonorrhoeae* and *C. trachomatis* in genitourinary specimens from men and women by a coamplification PCR assay. *J. Clin. Microbiol.* 1997; **35**: 1536–40.

10 Miyashita N, Iijima Y, Matsumoto A. Evaluation of the sensitivity and specificity of Polymerase Chain Reaction Test Kit, AMPLICOR *Chlamydia trachomatis*. *Microbiol. Immunol.* 1994; **38**: 81–5.

11 Longo MC, Berninger MS, Hartley JL. Use of uracil DNA glycosylase to control carry-over contamination in polymerase chain reactions. *Gene* 1990; **93**: 125–8.

12 Li Z, Yokoi S, Kawamura Y, Maeda S, Ezaki T, Deguchi T. Rapid detection of quinolone resistance-associated *gyrA* mutations in *Neisseria gonorrhoeae* with a LightCycler. *J. Infect. Chemother.* 2002; **8**: 145–50.

13 Zariffard MR, Saifuddin M, Sha BE, Spear GT. Detection of bacterial vaginosis-related organisms by real-time PCR for Lactobacilli, *Gardnerella vaginalis* and *Mycoplasma hominis*. *FEMS. Immunol. Med. Microbiol.* 2002; **34**: 277–81.

14 O'Neill HJ, Wyatt DE, Coyle PV, McCaughey C, Mitchell F. Real-time nested multiplex PCR for the detection of herpes simplex virus types 1 and 2 and *Varicella zoster* virus. *J. Med. Virol.* 2003; **71**: 557–60.

15 Hardick J, Yang S, Lin S, Duncan D, Gaydos C. Use of the Roche LightCycler instrument in a real-time PCR for *Trichomonas vaginalis* in urine samples from females and males. *J. Clin. Microbiol.* 2003; **41**: 5619–22.

16 Yoshida T, Deguchi T, Ito M *et al.* Quantitative detection of *Mycoplasma genitalium* from first-pass urine of men with urethritis and asymptomatic men by real-time PCR. *J. Clin. Microbiol.* 2002; **40**: 1451–5.

17 Deguchi T, Yoshida T, Yokoi S *et al.* Longitudinal quantitative detection by real-time PCR of *Mycoplasma genitalium* in fast-pass urine of men with recurrent nongonococcal urethritis. *J. Clin. Microbiol.* 2002; **40**: 3854–6.

18 Varela JA, Otero L, Garcia MJ *et al.* Trends in the prevalence of pathogens causing urethritis in Asturias, Spain, 1989–2000. *Sex. Transm. Dis.* 2003; **30**: 280–3.

19 Krieger JN. Trichomoniasis in men: old issues and new data. *Sex. Transm. Dis.* 1995; **22**: 83–96.

20 Takahashi S, Shimizu T, Takeyama K *et al.* Detection of human papillomavirus DNA on the external genitalia of healthy men and male patients with urethritis. *Sex. Transm. Dis.* 2003; **30**: 629–33.

J Infect Chemother (2007) 13:380–389
DOI 10.1007/s10156-007-0556-1

ORIGINAL ARTICLE

Yasushi Ohkusa · Tamie Sugawara

Application of an individual-based model with real data for transportation mode and location to pandemic influenza

Received: April 23, 2007 / Accepted: August 9, 2007

Abstract Currently, an individual-based model is a basic tool for creating a plan to prepare for the outbreak of pandemic influenza. However, even if we can construct the model as finely as possible, it cannot mimic the real world precisely. Therefore, we should use real data for transportation modes and locations, and simulate the diffusion of an infectious disease into that real data. In the present study, we obtained data on the transportation modes and locations of 0.88 million persons a day in the Tokyo metropolitan area. First, we defined the location of all individuals in the data set every 6 min. Second, we determined how many people they came in contact with in their household, in each area, and on the train, and then we assumed that a certain percentage of those contacted would become infected and transmit the disease. Data for natural history and other parameters were taken from previous research. The average number of contacts in each area was 51 748 (95% confidence intervals [CI],46 846–56 650]), at home it was 246 (95% CI, 232–260), and on the train it was 91 (95% CI, 81–101). The number of newly infected people was estimated to be 3032 on day 7 and 126 951 on day 10. The geographic diffusion on day 7, the day when the earliest response would have started, expanded to the whole of the Tokyo metropolitan area. We were able to realize the speed and geographic spread of infection with the highest reality. Therefore, we can use this model for making preparedness plans.

Key words Mathematical model · Pandemic influenza · Simulation

Introduction

Currently, individual-based models are basic tools used in creating plans to prepare for the outbreak of pandemic influenza[1–6] or a bioterrorism attack.[7] For example, the studies of Ferguson et al.[1] and Longini et al.,[2] two very famous studies which have been cited in the WHO containment strategy and the pandemic plan of the United States, both use such models. However, even if we can construct the model as finely as possible, it is just a model, not real, and it cannot mimic the real world precisely. Moreover, it cannot model the risk of infection when people commute by train, especially when trains are very crowded, as they can be in Tokyo and other large cities in Asia. Germann et al.[4] and Ferguson et al.[5] constructed a model for the United States and one for the United Kingdom, but they ignored the possible risk inherent in commuting. Therefore, we need to create a new model from the viewpoint of urban engineering, i.e., we should use real data for transportation modes and locations, and simulate the diffusion of an infectious disease into that real data.

Using a real data set and an individual-based model, we can trace the diffusion of disease from one arbitrarily chosen person to the whole of the metropolitan area day by day. We can construct a mathematical model for pandemic influenza so as to evaluate the effectiveness of school or workplace closure and the risk of commuting on crowded trains, or to measure the necessary distance for area quarantine. For example, we can measure the distribution of diffusion when we find clusters in a small area. We call this model a real individual-based model (hereafter, Ribm) and we propose that this is the best mathematical model for planning to prepare for pandemic influenza at this time.

Similar studies have already been performed. For example, Eubank et al.[8] confirmed the small worldness using actual location data in Portland, a city which has a population of 1.6 million, and their group applied this to a bioterrorist attack of smallpox.[9] However, they ignored contact within transportation devices, including trains. Conversely, in Japan, another study only used data about contact in commuter trains,[10] but it ignored contact in other places, e.g., households, schools, and workplaces. Therefore, data which include both location and transportation seem to be the most important and useful, but such data have not been used so far. Differences among households, schools, work-

Y. Ohkusa · (✉) · T. Sugawara
Infectious Disease Surveillance Center, National Institution of Infectious Disease, 1-23-1 Toyama, Shinjuku-ku, Tokyo 162-8640, Japan
Tel. +81-3-5285-1111 (ext.2057); Fax + 81-3-5285-1129
e-mail: ohkusa@nih.go.jp

places, and trains are also important in the sense of frequency and closeness of contact. In this research, we were permitted to use the Person-Trip data of the Tokyo metropolitan area (hereafter, PT data) so as to make a preparedness plan for pandemic influenza and/or bioterrorism. We focus especially on how pandemic influenza would diffuse through the Tokyo metropolitan area when the first case is introduced to Japan.

Methods

The PT data[10] were collected in 1998 and included data on all transportation modes, such as cars, trains, buses, bicycles, and walking, and the locations of 0.88 million persons a day in the Tokyo metropolitan area (which has a population of 33 million). In other words, about 2.7% of the population was randomly chosen and their actual behavior was surveyed for urban planning. This set of data includes, all transportation modes and locations in 1 day for all family members over 5 years old. The types of places were defined as household, school, workplace, and others. We were able to identify the area where these people are in terms of 1648 zones, each of which is 1 km^2 on average. Moreover, we know the name of the station where the people get the train and where they get off, and the timing.

At first, we defined the location of all individuals in the PT data every 6 min. Location was defined as at home, the zone they are in, and train which they take. Second, we determined how many people they came in contact with in their household, in each area, and on the train. Then, we examined whether the distribution of contact in the household, area, and train were scale-free. Namely, we estimated the exponential distribution as $P(k) = ak^{-b}$, where k is the number of contacts, and P(k) is the probability. If b is significantly positive, it means that it is scale-free. To estimate b, we adopted two methods.

One procedure was regression log transformation of the cumulative distribution: $C(k) = ak^{1-b}/(1-b)$, $\log C(k) = \log(a/(1-b)) + (1-b)\log k$ on $\log k$, and 1 minus the estimated coefficient of $\log k$, is the estimator of b. Another procedure was a regression log transformation of the probability density function: $\log P(k) = \log a - b \log k$ on $\log k$ and minus the estimated coefficient of $\log k$ is the estimator of b. The probability density function is estimated by the slope of the cumulative distribution function, which is observable.

So as to see the small worldness visually, we also performed a simulation of pandemic influenza on the PT data by assuming that a certain percentage of those contacted would become infected and transmit the disease. In this simulation, 0.88 million persons behave as the data states and come in contact with each other every day. The probability of infection, of course, depends on the type of place, such as household, school, workplace, and train, based on how close the proximity of the people in that area is.

Transmission in each area or on the train is assumed to occur in a 1-m circle. As the area is defined by zones which are 1 km^2 on average, contact in the area is estimated to be $n \times 3.14 \times 37.0/1000^2$, where n is the number of people in the same area at the same time in the PT data and 37.0 is the reciprocal number of the sampling rate, 2.7%. Similarly, contact in the train is defined as $n \times 3.14 \times 37.0/1200$, where n is the number of people on the same train at the same time in the PT data and 1200 indicates the total area of the train, assuming a carriage has an area of 4 m × 30 m and each train has 10 carriages. Because there have been no studies of transmission in crowded trains, though infection in airplanes has been studied,[11] we had to assume the probability of transmission; it was assumed to be 100α% if someone was around a symptomatic patient for more than 1 h within a distance of less than 1 m, where α is infectiousness at home or in that area. If the person stayed for less than 1 h, the probability was assumed to decline proportionally according to the duration. For example, if someone were to stay

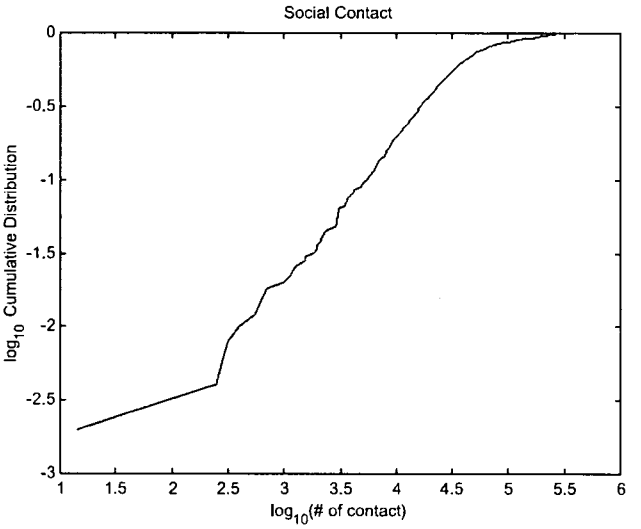

Fig. 1. Cumulative distribution function of contact in the area

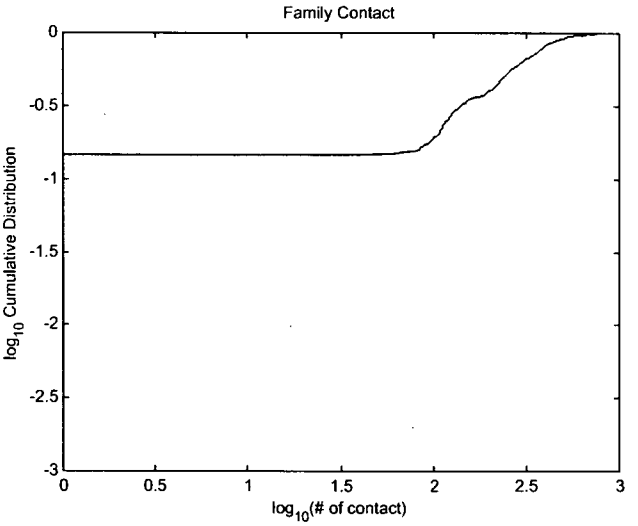

Fig. 2. Cumulative distribution function of contact at home

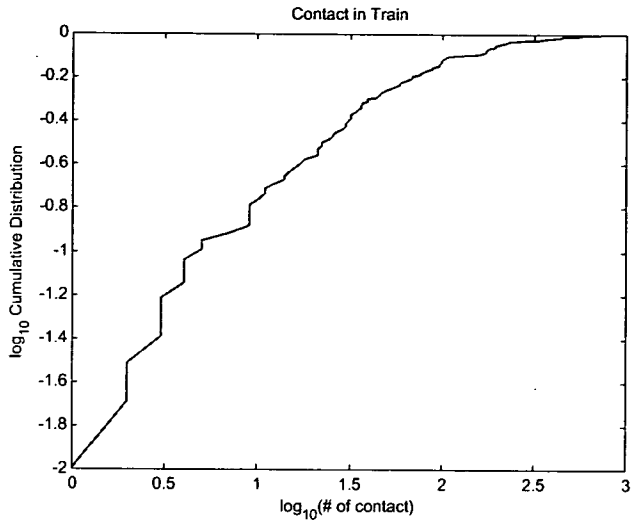

Fig. 3. Cumulative distribution function of contact on the train

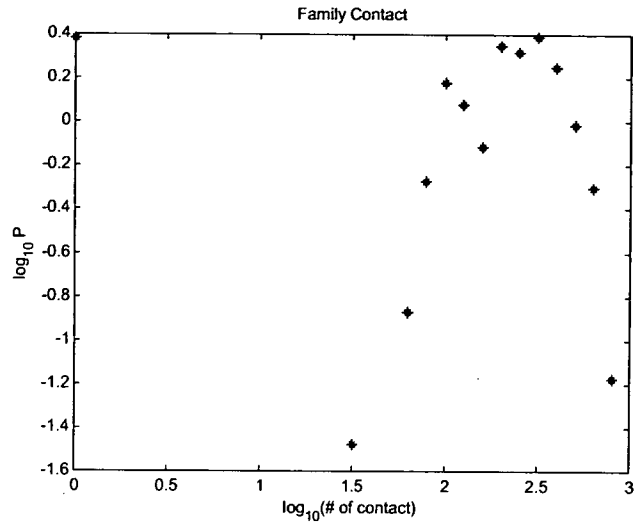

Fig. 5. Histogram of contact at home

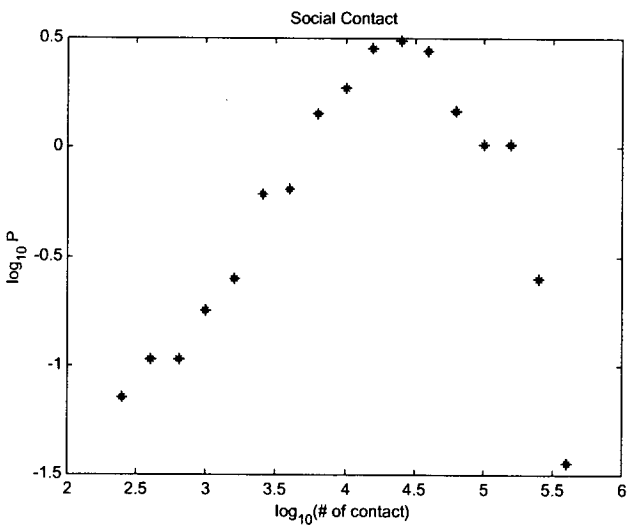

Fig. 4. Histogram of contact in the area

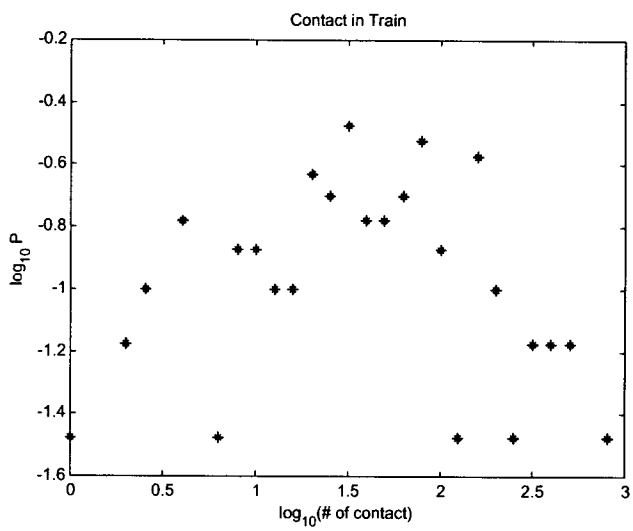

Fig. 6. Histogram of contact on the train

around a patient for 6 min, the probability of infection was assumed to be $10\alpha\%$.

Data for the natural history of the disease, the period when the patient is infectious, and the incidence and infectiousness of asymptomatic patients, as well as the withdraw rate were taken from previous research.[3,4] The α value was determined by these parameters, and thus the basic reproduction number (R_0) at home or in the area was the same as that in the previous research, in which R_0 was assumed to be 1.6–2.4. In other words, this model assumes a higher R_0 than the previous research, due to taking infection in crowded trains into consideration.

A simulation was performed with the following scenario: the initial patient was infected in an affected area outside Japan on day 1, then s/he came back to Japan on day 3, and s/he infected her/his family at Hachiouji. Her/his workplace was proposed to be at Marunouchi and so s/he commuted by train on day 4 when s/he was exhibiting symptoms. On day 5, s/he visited a doctor. The doctor suspected H5N1 from her/his travel history and ordered tests from the local public laboratory. At least 1 day is necessary to obtain the test results, and thus any response to contain the spread of the disease would start on day 6 if decisions were made as soon as possible.

Finally, so as to evaluate countermeasures, we used voluntary staying at home as one example of a countermeasure. In this countermeasure, we assumed that the person would reduce 40% of their commute by train and

80% of other activities, including school or shopping, and this would start on day 6 or 7.

Results

We estimated the number of contacts using 638 individuals who were randomly chosen from the whole of the PT data. This number of examined individuals was chosen because of limitations in computer resources. The average number of contacts in each area was 51 748 (95% confidence intervals [CI], 46 846–56 650), at home it was 246 (95% CI, 232–260), and on the train it was 91 (95% CI, 81–101). Figures 1 through 3 show the cumulative distribution of the number of contacts in the area, at home, and on the train, respectively Figures 4 through 6 show the probability density function from the histograms, while Figs. 7 through 9 show the probability density function from the slope of the cumulative distribution.

Table 1. summarizes the estimation results from the cumulative distribution function, and the estimation results from the probability density function through the slope of cumulative distribution are shown in Table 2. All estimates for b, which is the power parameter, were significantly positive in all areas, households, and trains. The estimated coefficients were 0.25, 0.57, and 0.33, respectively, (Table 1), and 0.75, 0.69, and 0.83, respectively (Table 2).

Figures 10–17 show the data from day 3, when the initial patient came back to Japan, to day 10, when the computational burden exceeded our computer resources. The maps in these Figs. were made by ArcGIS with map information

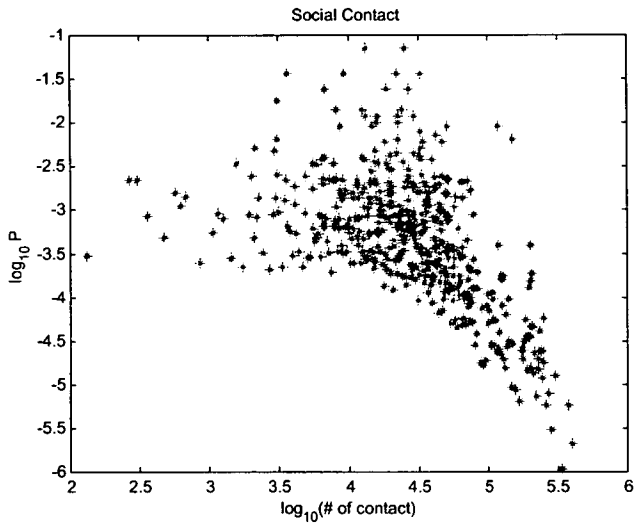

Fig. 7. Probability density function of contact in the area

Table 1. Estimation results from the cumulative distribution function

Contact place	Estimated coefficient	*P* value*	Estimated coefficient of b
Area	0.7498115	0.000	0.25
Household	0.4348235	0.000	0.57
Train	0.6774273	0.000	0.33

* *P* value for the null hypothesis that b = 0

Table 2. Estimation results from the probability density function

Contact place	Estimated coefficient	*P* value*	Estimated coefficient of b
Area	−0.7528538	0.000	0.75
Household	−0.6857427	0.000	0.69
Train	−0.8329078	0.000	0.83

* *P* value for the null hypothesis that b = 0

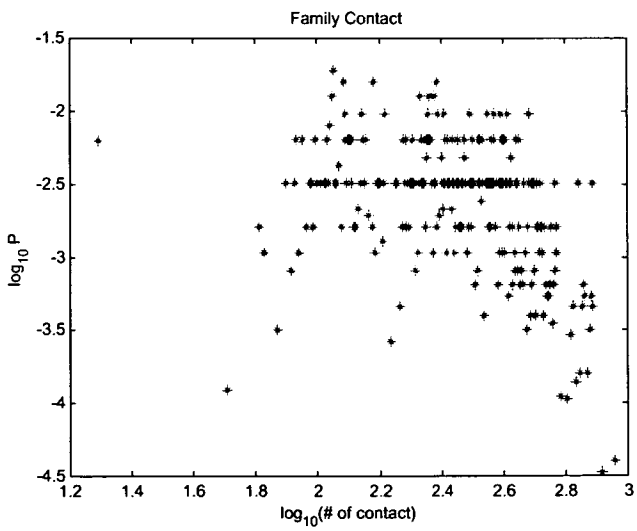

Fig. 8. Probability density function of contact at home

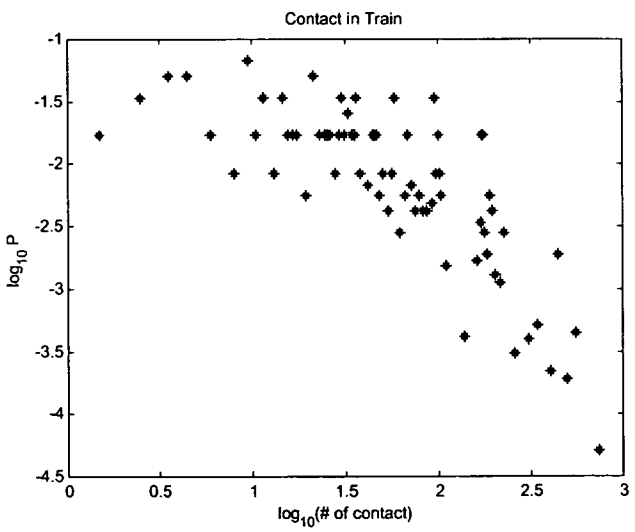

Fig. 9. Probability density function of contact on the train

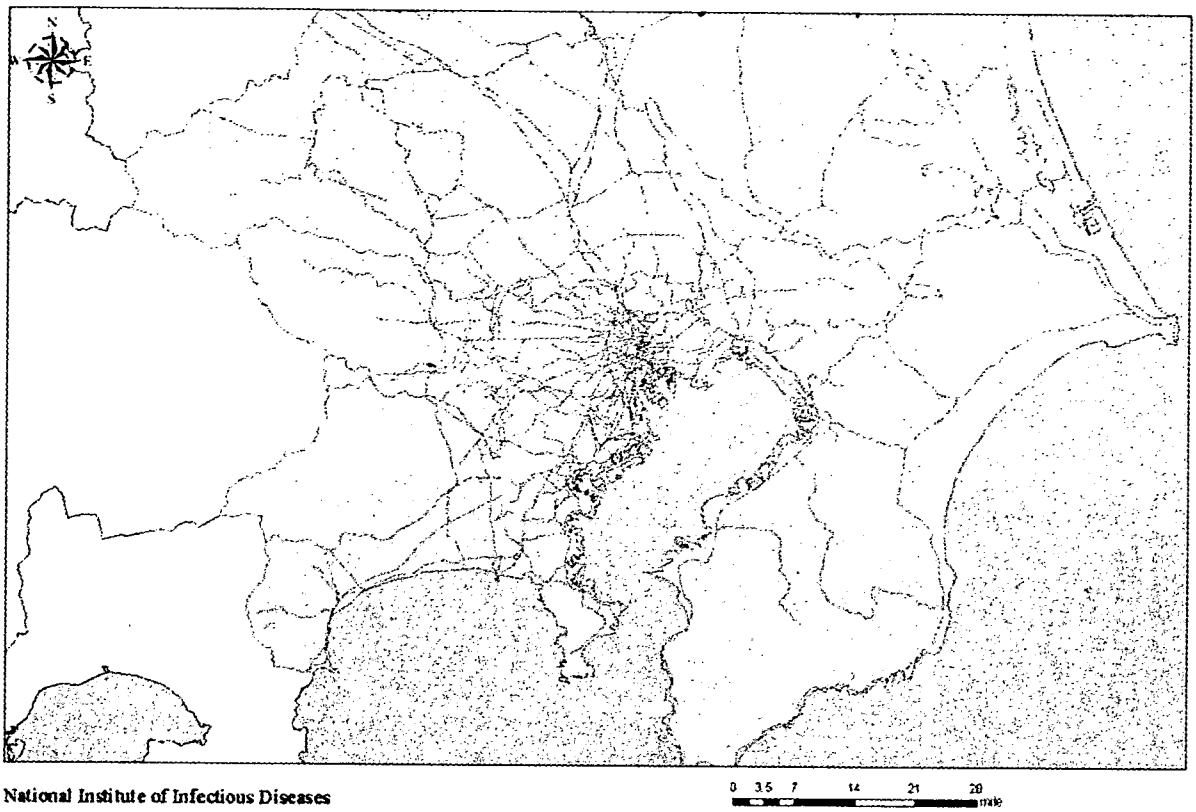

Fig. 10. Simulation result of the infection on day 3

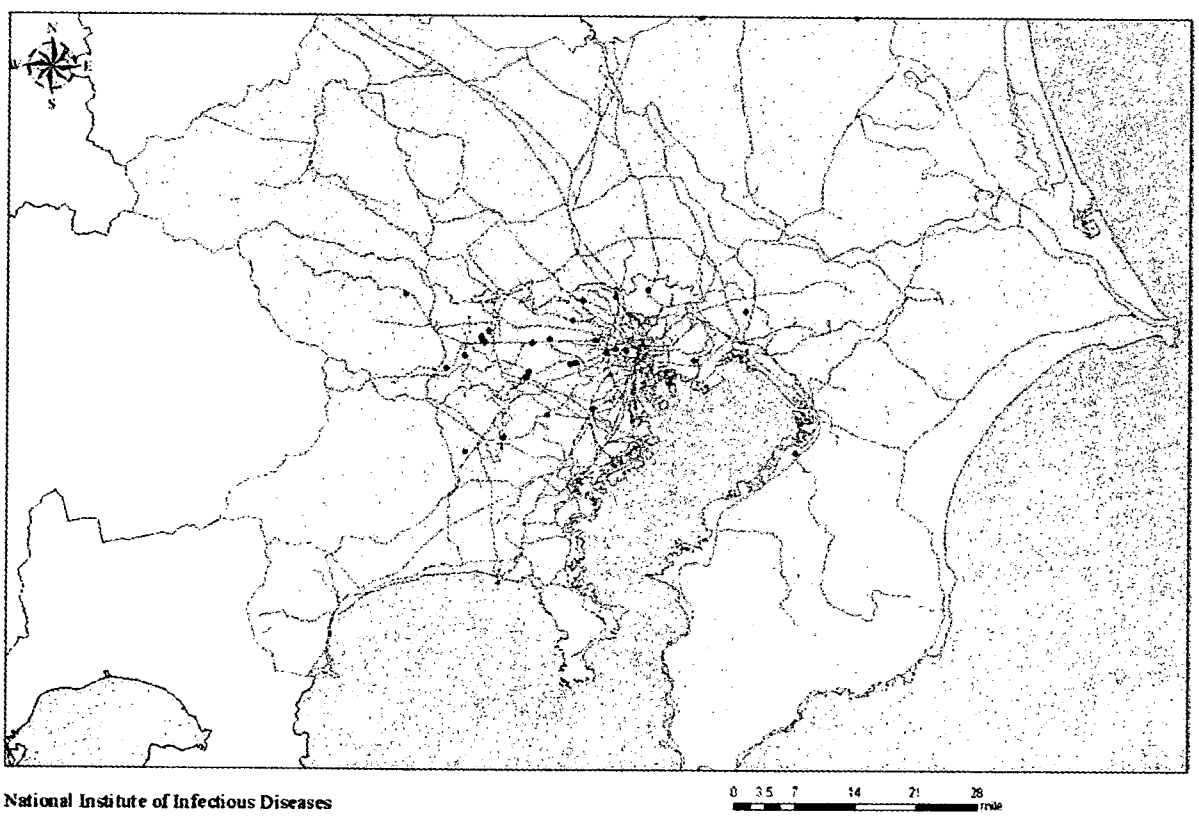

Fig. 11. Simulation result of the infection on day 4

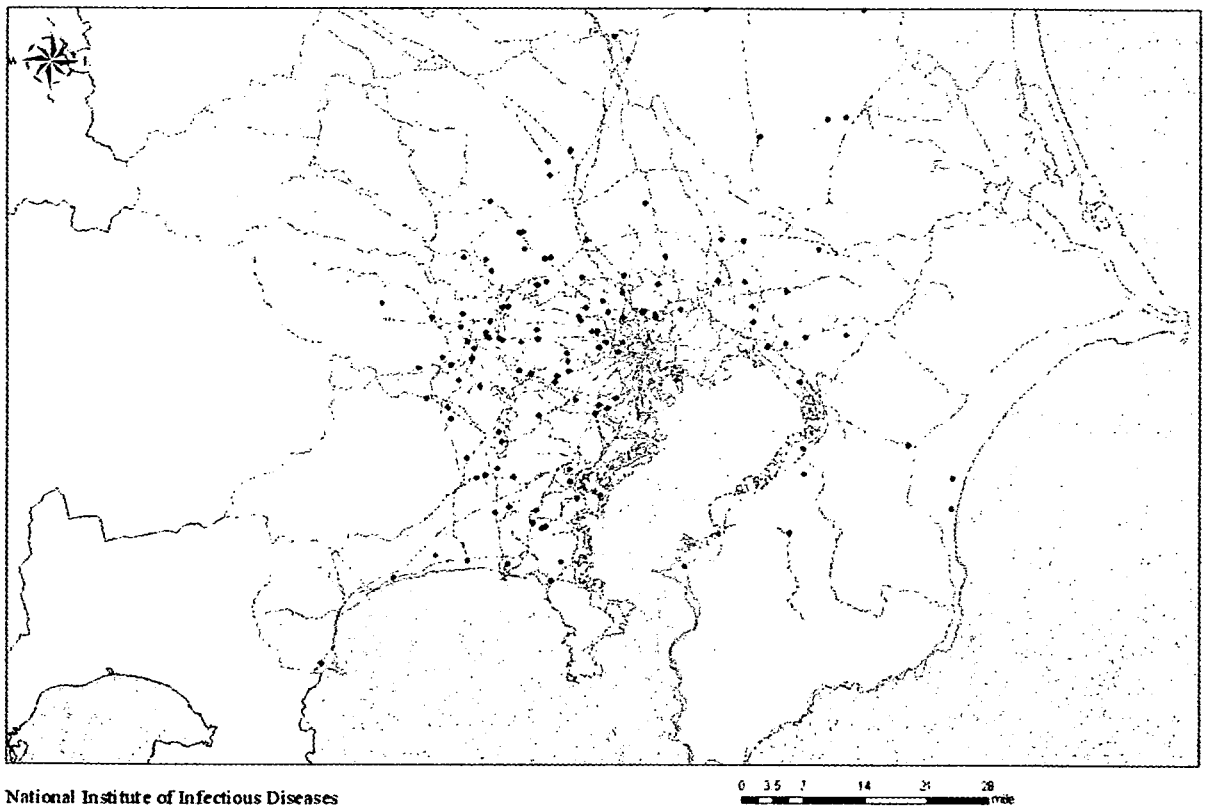

Fig. 12. Simulation result of the infection on day 5

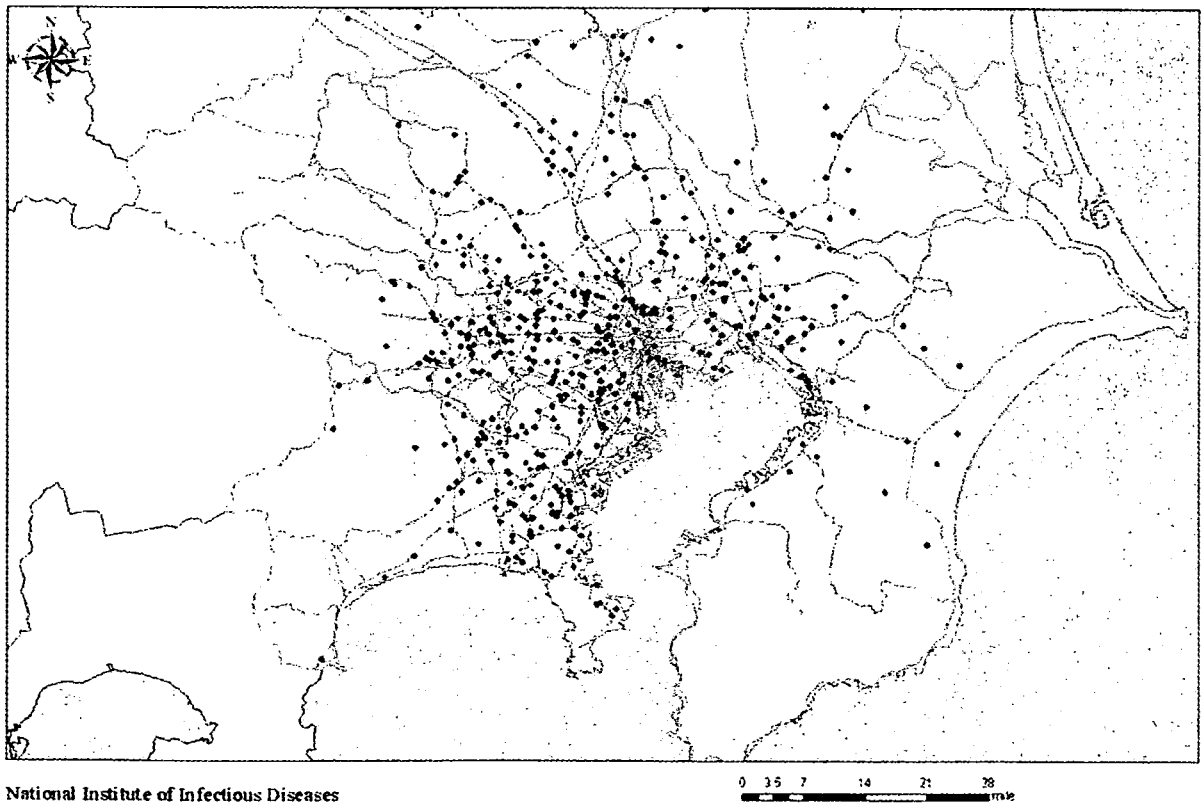

Fig. 13. Simulation result of the infection on day 6

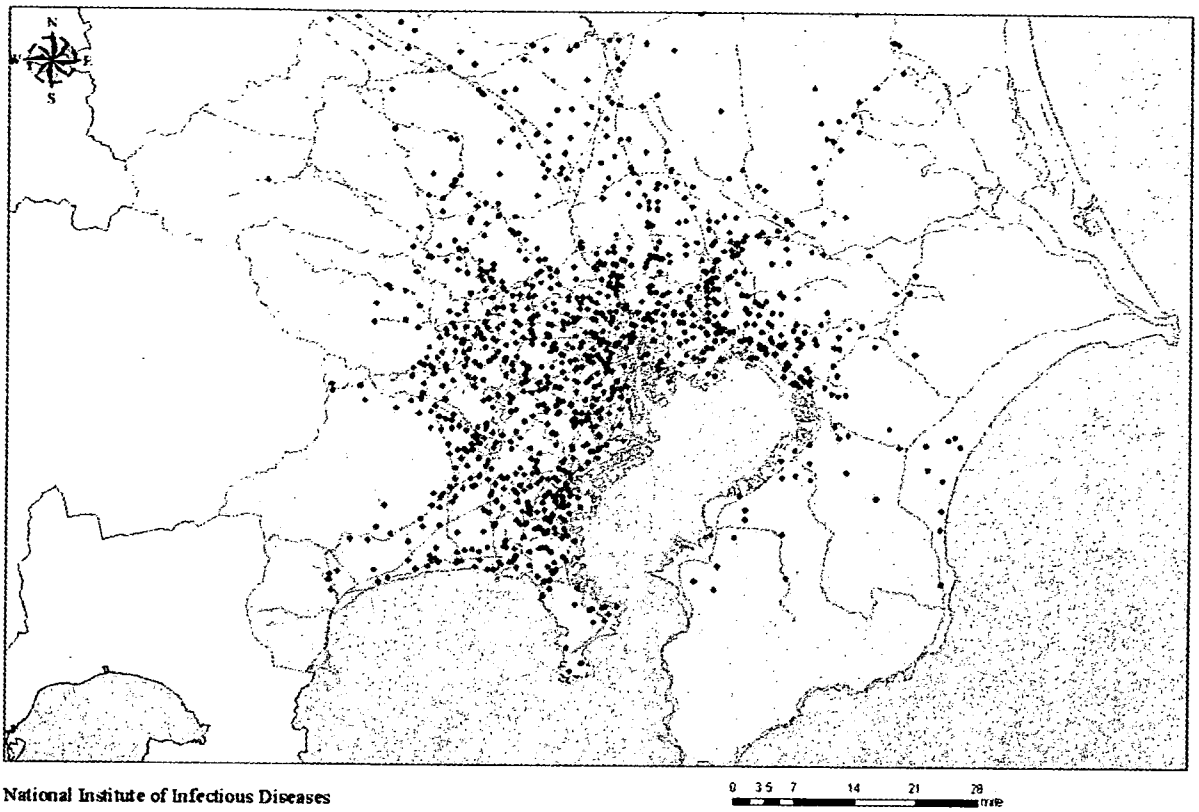

Fig. 14. Simulation result of the infection on day 7

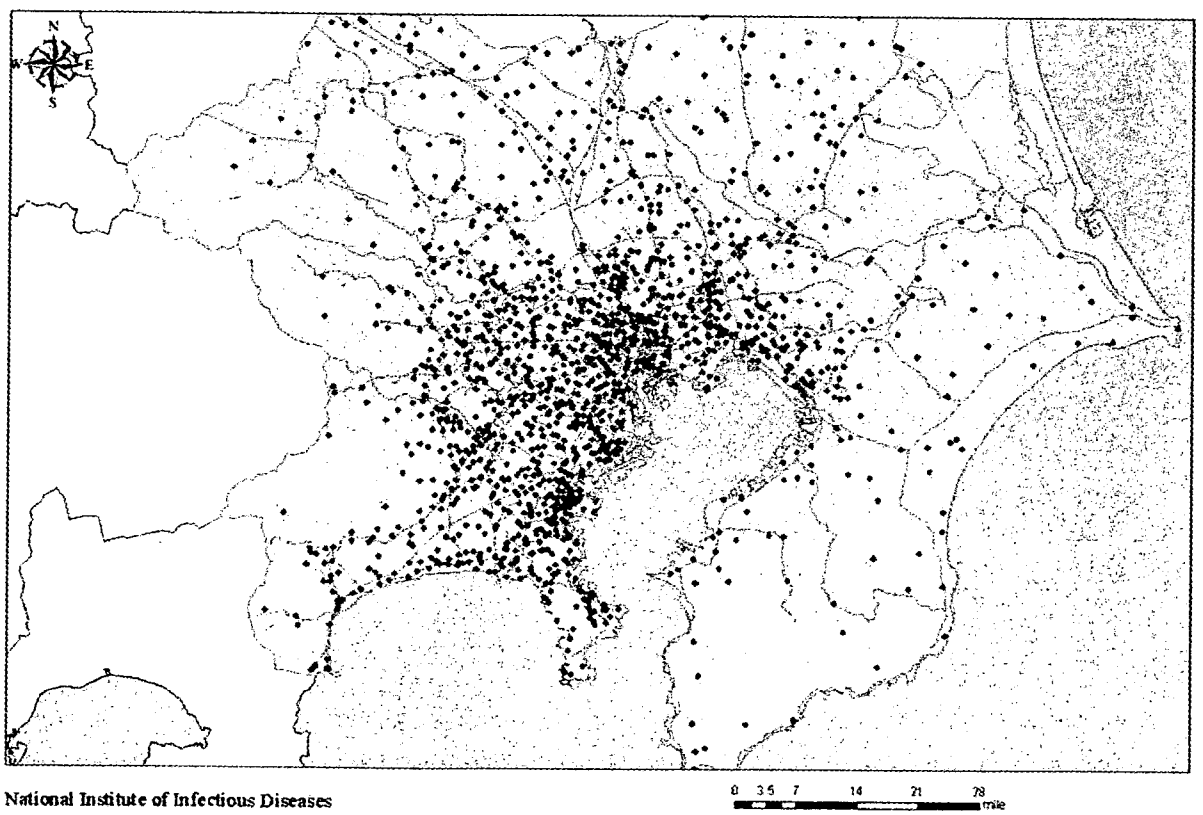

Fig. 15. Simulation result of the infection on day 8

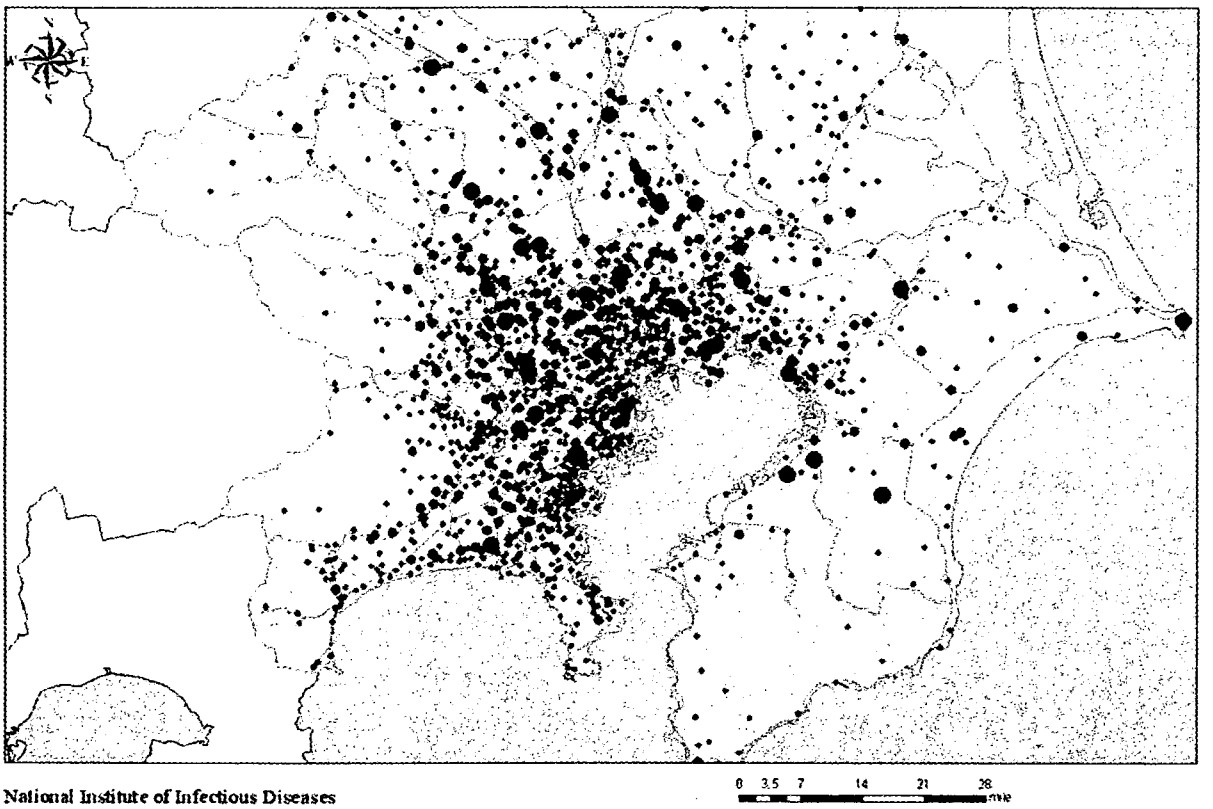

Fig. 16. Simulation result of the infection on day 9

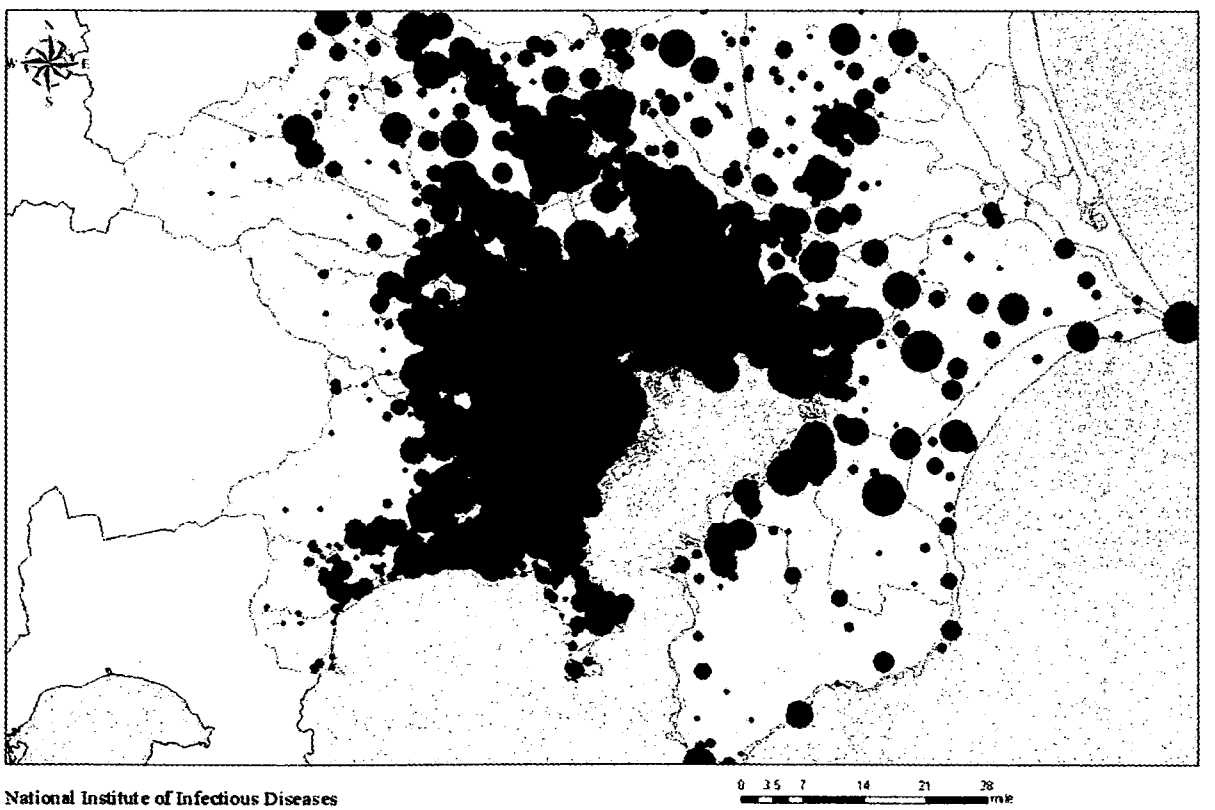

Fig. 17. Simulation result of the infection on day 10

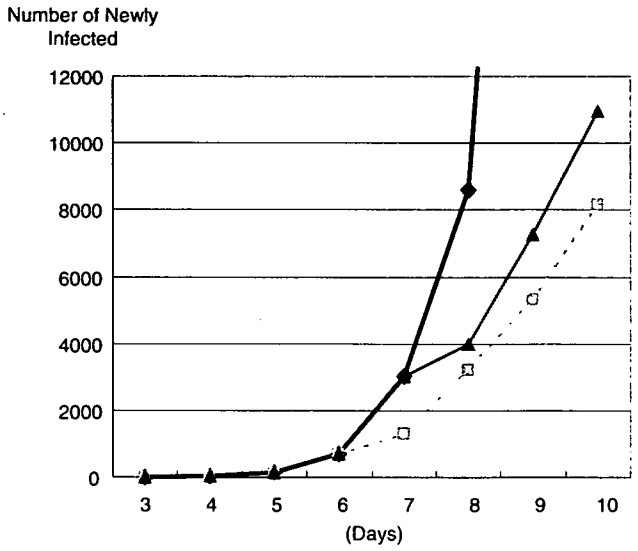

Fig. 18. Effect of voluntary staying at home. *Diamonds*, no intervention; *squares*, voluntary staying at home started day 6; *triangles*, voluntary staying at home started day 7

from numerical map 25000 produced by the Geographical Survey Institution, the Ministry of Land, Infrastructure and Transport, Japan, and map information by prefecture produced by ESRI Japan.

Circles in the figures indicate the newly infected people at their home address when they were infected. The sizes of the circles indicate the numbers of newly infected people. The number of newly infected people was estimated to be 3032 on day 7 and 126951 on day 10.

Figure 18 shows the epidemic curves of one "no intervention" subject (i.e., and two control subjects. For the no intervention subject the number of infected people was huge after day 7, so, these data are not shown.

Discussion

Because the actual number of contacts in Japan is not known, and this number is not well known outside Japan, our finding that social contact is scale-free with low power must be very valuable. Even though the two estimators, from the cumulative distribution and the probability density function through the slope of the cumulative distribution, were slightly different, they are lower than one and thus show low power. So far, the power of in an actual society is estimated as 1.9 to 3.5 in sexual partners or contact,[12,13] but it has never been estimated for contact in areas, trains, or at home. Therefore our findings about lower but significant power in usual activity are quite important.

We proposed that the initial patient visited a doctor on day 5 and that the response started as soon as possible, on day 7. According to the geographic diffusion shown in Fig. 14, the infection had expanded to the whole of the Tokyo metropolitan area by day 7. Therefore area quarantine would be difficult to perform, and 5- to 20-km radius area quarantine, which has been proposed in previous studies[14] would fail to contain the disease.

The figures do not indicate any infections in the areas surrounding the Tokyo metropolitan area; such as Gunma, Tochigi, Yamanashi, and Shizuoka prefectures and the northern area of Ibaragi prefecture. However this does not mean that there are no infections in these areas. It is simply because the PT data we used do not cover these areas and thus our simulation model cannot predict any infections in these areas. For the same reason, our results do not show any infection in other large cities outside the Tokyo metropolitan area; such as Osaka, Nagoya, or Fukuoka. We can easily assume, however, that the situation would be almost the same in other large cities with a few days or even just a few hours of delay.

On the other hand, in local cities, transportation by train, especially commuting, is not as common as it is in the Tokyo metropolitan area, so disease transmission is slower in local cities than in the Tokyo metropolitan area. Therefore, we may have some chances to contain an outbreak using an area quarantine strategy in these local cities.

However, voluntary staying at home is more effective than a quarantine strategy. It can reduce the number of those infected to about 1/13 compared with the number infected without the implementation of such a policy. Moreover, its cost is estimated to be minimal. This policy is recommended by the preparedness plan.

We note that there are many limitations in our simulation. First of all, many parameters, such as the width of the train or area of the zone, or infectiousness, were assumed. Thus, we may have overestimated or underestimated the number of patients. For example, though we assumed that the area of a zone was 1 km^2, the area where people are present is much smaller than the whole area of the zone. In this case, the amount of contact and thus the number of patients may have been underestimated. In general, such an uncertainty is fixed by wide sensitivity analysis. However, our model is too huge to perform sensitivity analysis and it would require a long time due to the limitation of computer resources. Therefore we cannot perform sensitivity analysis yet. Such a robustness check is the next challenge. As this model is stochastic, each simulation must have different results and the number of patients is assumed to have a broad distribution. However, even if the number of patients may be underestimated or overestimated, the speed of spread does not seem to be greatly affected by the set parameters of the estimated number of patients, because significant small worldness was confirmed, as shown in Tables 1 and 2. In this sense, estimation of the number of patients itself is not so important, and the speed of spread is more important for this model. As Figs. 10–17 show, the speed of spread may be much higher than that shown by our image so far because of its small worldness, and this finding is the most important message of this simulation.

Second, the data we used were for the behavior of 0.88 million persons, but only for 1 day. In general, we change our behavior slightly day by day. Typically, we behave in

different patterns on the weekend in comparison with weekdays. Therefore, the actual contact pattern and thus the numbers of contacted persons are not the same every day. However, this model does not incorporate such an obvious fact. This reduces the transmission efficiency of the model in diffusing pandemic influenza.

Third, we did not examine the effect of countermeasures such as antiviral prophylaxis, school closure, and/or vaccination. In principle, however, we can apply this model to the issue of countermeasures. This application is one of the next challenges.

Conclusion

In this study, we used actual data for transportation and location combined with an ibm, and applied the data to pandemic influenza. We were able to realize the speed and geographic spread of infection with the highest reality. Therefore, we can develop the Ribm as a useful model which we can use in making preparedness plans. So as to be more useful, we have to extend the Ribm to local cities with long-distance transportation by airplane or the bullet train, as well as the Tokyo metropolitan area. Unfortunately, an Ribm has not been adopted in the preparedness plan for pandemic influenza[15] so far, but we hope to use an Ribm to improve the plan.

Acknowledgments We appreciate the Traffic Planning Council in the Tokyo Metropolitan Area for permission to use the data.

References

1. Ferguson NM, Cummings DA, Cauchemez S, Fraser C, Riley S, Meeyai A, et al. Strategies for containing an emerging influenza pandemic in Southeast Asia. Nature 2005;437:209–14.
2. Longini IM Jr, Nizam A, Xu S, Ungchusak K, Hanshaoworakul W, Cummings DA, et al. Containing pandemic influenza at the source. Science 2005;309:1083–7.
3. Ohkusa Y, Maeda H, Aihara K. Evaluation of pandemic plan using individual based model; the Joint Meeting of Japan and Korea Biological Mathematics at Fukuoka, 2006.
4. Germann TC, Kadau K, Longini IM Jr, Macken CA. Mitigation strategies for pandemic influenza in the United States. Proc Natl Acad Sci USA 2006;6:5935–40.
5. Ferguson NM, Cummings DA, Fraser C, Cajka JC, Cooley PC, Burke DS. Strategies for mitigating an influenza pandemic. Nature 2006;103:5935–40.
6. Glass RJ, Glass LM, Beyeler WE, Min HJ. Targeted social distancing designs for pandemic influenza. Emerging Infection Diseases 2006;12.
7. Ohkusa Y. An evaluation of counter measures for smallpox outbreak using an individual based model and taking into consideration the limitation of human resources of public health workers (in Japanese). Medicine and Society 2007;16:275–84.
8. Eubank S, et al. Modeling disease outbreaks in realistic urban social networks. Nature 2004;429:180–4.
9. Barrett CL, Eubank SG, Smith JP. If smallpox strikes Portland. Sci Am 2005;292:42–9.
10. Guide for person-trip data in Tokyo metropolitan area. Tokyo: Tokyo Metropolitan Traffic Planning Council; 2004.
11. Mangili A, Gendreau MA. Transmission of infectious diseases during commercial air travel. Lancet 2005;365:989–96.
12. Newman MEJ. The structure and function of complex networks. SIAM Review of Society of Applied Mathematic 2003;45:167–256.
13. Albert R, Barabasi AL. Statistical mechanics of complex networks. Review of Modern Physics 2002;74:47–97.
14. Expert Advisory Meeting for Pandemic Influenza (2007 Guideline for pandemic influenza (after phase 4 version). March 26, 2007.